Constraining Dissipative Dark Matter Self-Interactions

Rouven Essig,[1] Samuel D. McDermott,[2] Hai-Bo Yu,[3] and Yi-Ming Zhong[4,*]
[1]C.N. Yang Institute for Theoretical Physics, Stony Brook University, Stony Brook, New York 11794, USA
[2]Fermi National Accelerator Laboratory, Center for Particle Astrophysics, Batavia, Illinois 92376, USA
[3]Department of Physics and Astronomy, University of California, Riverside, California 92521, USA
[4]Physics Department, Boston University, Boston, Massachusetts 02215, USA

(Received 1 October 2018; published 18 September 2019)

We study the gravothermal evolution of dark matter halos in the presence of dissipative dark matter self-interactions. Dissipative interactions are present in many particle-physics realizations of the dark-sector paradigm and can significantly accelerate the gravothermal collapse of halos compared to purely elastic dark matter self-interactions. This is the case even when the dissipative interaction timescale is longer than the free-fall time of the halo. Using a semianalytical fluid model calibrated with isolated and cosmological N-body simulations, we calculate the evolution of the halo properties—including its density profile and velocity dispersion profile—as well as the core-collapse time as a function of the particle model parameters that describe the interactions. A key property is that the inner density profile at late times becomes cuspy again. Using 18 dwarf galaxies that exhibit a corelike dark matter density profile, we derive constraints on the strength of the dissipative interactions and the energy loss per collision.

DOI: 10.1103/PhysRevLett.123.121102

Introduction.—The elusive nature of dark matter (DM) in terrestrial experiments combined with hints for nontrivial dynamics from astrophysical systems has led to the dark sector paradigm: the DM may be connected to a plethora of hidden particles with their own interactions; see Refs. [1–3] for overviews. These dark-sector interactions may modify the formation and evolution of DM halos and alter their inner structure. Astrophysical observations can in turn provide important tests on the microscopic physics in the dark sector.

In this Letter, we explore observational consequences of a generic dark-sector model, where DM particles have both elastic and dissipative self-interactions. Self-interacting DM (SIDM) has been proposed to solve long-standing issues of the prevailing cold DM model on galactic scales; see Ref. [4] for a review. Most SIDM studies focus on the elastic scattering limit. However, in many particle physics realizations of SIDM [5–15], DM particles also have dissipative collisions. We show that observations of constant DM density cores in many dwarf galaxies can be used to test dissipative DM self-interactions.

A finite self-gravitating system has negative heat capacity, and the evolution of an SIDM halo culminates in the "gravothermal catastrophe" [16]: over sufficiently long timescales, the inner core ultimately experiences gravitational collapse and a cuspy density profile reappears [17]. If this were to occur, SIDM would, in fact, fail to explain the low-density cores exhibited in many dwarf and low surface brightness (LSB) galaxies [18–25]. Interestingly, if the self-interactions are exclusively elastic, halo core collapse only occurs within the age of the Universe for self-scattering cross section per unit mass $\sigma/m \gtrsim 10$–$50\ \mathrm{cm}^2/\mathrm{g}$ [26,27], whereas $\sigma/m \sim \mathcal{O}(1)\ \mathrm{cm}^2/\mathrm{g}$ is sufficient to explain stellar kinematics in dwarfs [26–36]. However, in the presence of dissipative interactions, the gravothermal evolution of an SIDM halo can be accelerated significantly, as we will show.

We focus on the "mild cooling regime," in which the cooling timescale is longer than the free-fall time of the halo. In this case, the halo mostly stays in hydrostatic equilibrium and contracts as a whole without fragmentation, as opposed to situations with strong cooling [37–41]. After introducing a physical model to capture the bulk cooling, we perform numerical simulations to trace the evolution of the halo and calibrate the results against both isolated and cosmological N-body simulations. Finally, we derive strong limits on the strength of dissipative interactions in the dark sector. In Supplemental Material [42], we provide additional details and results to further support our main text.

Methodology.—To understand halo evolution in the presence of dissipative interactions, we employ a semi-analytical fluid model, which has been used to study globular clusters [43–45] and halos consisting of SIDM without dissipation [46–50]. Since this method is computationally inexpensive, we are able to scan a wide range of parameter space. Moreover, it can resolve the very inner regions of the simulated halo.

For an isolated halo, we assume spherical symmetry and use the following set of transport equations to describe the gravothermal evolution in the radial direction

$$\frac{\partial}{\partial r}M = 4\pi r^2\rho, \qquad \frac{\partial}{\partial r}(\rho\nu^2) = -\frac{GM\rho}{r^2},$$
$$\frac{\rho\nu^2}{\gamma-1}\left(\frac{\partial}{\partial t}\right)_M \ln\frac{\nu^2}{\rho^{\gamma-1}} = -\frac{1}{4\pi r^2}\frac{\partial L}{\partial r} - C, \qquad (1)$$

where $M(r,t)$ is the fluid mass enclosed within radius r at a time t, $\rho(r,t)$ is the local density, $\nu(r,t)$ is the one-dimensional velocity dispersion, $L(r,t)$ is the luminosity, $C(r,t)$ is the volumetric bulk cooling rate, G is the gravitational constant, and $(\partial_t)_M$ denotes the Lagrangian time derivative. The temperature is related to ν as $m\nu^2 = k_B T$, where k_B is the Boltzmann constant. We assume the DM particle is monatomic and set the adiabatic index $\gamma = 5/3$. The elastic and dissipative interactions are encoded in the conduction $\partial L/\partial r$ and the cooling term C, respectively. In this work, we assume both the elastic and inelastic cross sections are independent of the DM velocity.

DM elastic self-scattering allows radial heat conduction. This can be characterized by comparing the mean free path $\lambda = 1/n\sigma$, where n is the local number density and σ is the cross section, to the scale height $H = \sqrt{\nu^2/4\pi G\rho}$. The ratio of λ to H is the Knudsen number, $Kn \equiv \lambda/H$, which indicates the importance of heat conduction induced by elastic scattering. We refer to regions with $Kn > 1$ ($Kn < 1$) as long-mean-free-path (short-mean-free-path) regions. Note that $Kn \approx t_r/t_{\rm dy}$, where $t_r \approx \lambda/\nu$ is the local relaxation time for the elastic scattering and $t_{\rm dy} = H/\nu$ is the dynamical time of the halo. The luminosity L is a function of the temperature gradient $L/4\pi r^2 = -\kappa\partial T/\partial r$, where the conductivity $\kappa = (\kappa_{\rm lmfp}^{-1} + \kappa_{\rm smfp}^{-1})^{-1}$ reduces to the conductivity of the long-mean-free-path ($\kappa_{\rm lmfp}$) and short-mean-free-path ($\kappa_{\rm smfp}$) regions in the appropriate limits, i.e., $\kappa_{\rm lmfp} = (3\beta/2)nH^2k_B/t_r \simeq 0.27\beta n\nu^3\sigma k_B/(Gm)$, and $\kappa_{\rm smfp} = (75\pi/256)n\lambda^2 k_B/t_r \simeq 2.1\nu k_B/\sigma$ [47–50]. We determine the numerical factor β in $\kappa_{\rm lmfp}$ by calibrating the fluid model with N-body simulations. In this work, we have tested $\beta = 0.75$, 0.60, and 0.45 for isolated [49] and cosmological [27] N-body simulations with purely elastic DM self-interactions. Moreover, we have checked our fluid-model predictions ($\beta = 0.60$) with recent dissipative SIDM N-body simulations [51] and find good overall agreement; see the Supplemental Material [42] for details.

Since we assume the energy released during the dissipative collision is not reabsorbed by DM particles in the halo, the cooling rate C appears as a bulk term in Eq. (1), which can be written as a function of the model parameters,

$$C = \left\langle\frac{nE_{\rm loss}}{t_r'}\right\rangle = \rho^2\frac{\sigma'}{m}\frac{4\nu\nu_{\rm loss}^2}{\sqrt{\pi}}\left(1+\frac{\nu_{\rm loss}^2}{\nu^2}\right)e^{-(\nu_{\rm loss}^2/\nu^2)}, \qquad (2)$$

where $\nu_{\rm loss} \equiv \sqrt{E_{\rm loss}/m}$ is the "velocity loss" that parametrizes the energy loss per collision; σ' is the cross section of the dissipative interaction, and $t_r' \equiv 1/(n\sigma' v_{\rm rel})$ is the relaxation time with respect to the relative velocity of the two incoming particles, $v_{\rm rel}$; we take the thermal average $\langle\cdot\rangle$ with respect to the Boltzmann distribution of $v_{\rm rel}$ while restricting inelastic scattering to particles whose kinetic energy exceeds $E_{\rm loss}$, i.e., $v_{\rm rel} \geq 2\nu_{\rm loss}$. This model of cooling captures the essential features of dissipative interactions.

We solve Eq. (1) with the boundary conditions at $t = 0$ of $M = L = 0$ for the inner boundary and $L = 0$ for the outer boundary. We assume the initial halo mass distribution follows an NFW profile [52], $\rho(r) = \rho_s r_s^3/r(r+r_s)^2$, where ρ_s and r_s are the scale density and radius, respectively. In our simulations, we reformulate Eq. (1) in terms of a set of dimensionless variables based on r_s and ρ_s and follow the numerical procedure in Refs. [48,50]; see the Supplemental Material [42].

Gravothermal evolution.—To illustrate the effect of the dissipative interactions, we consider a dwarf halo with mass $8\times10^{10}\ M_\odot$ and characteristic halo parameters $r_s = 6.5$ kpc and $\rho_s = 1.28\times10^7\ M_\odot/{\rm kpc}^3$. Reference [33] took this NFW halo as an outer boundary condition to find the SIDM fit to the galactic rotation curve of LSB F583-1, which exhibits a cored density profile. We take $\sigma/m = 3\ {\rm cm}^2/{\rm g}$ as in Ref. [33] and consider $\sigma' = 0$ as well as $\sigma' = \sigma$ and

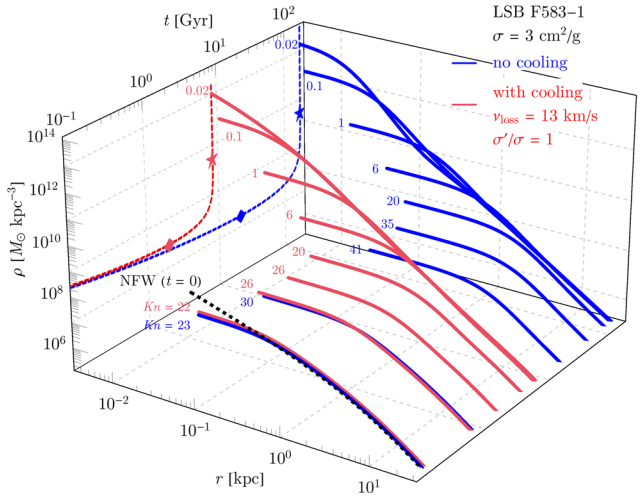

FIG. 1. The evolution of the density profiles for an SIDM halo, LSB F583-1, assuming purely elastic DM self-interactions ("no cooling," blue) and self-interactions with an additional dissipative interaction ("with cooling," red). Numbers show the Knudsen number for the innermost shell at a given time. We project the evolution of the density of the innermost shell on to the $\rho - t$ plane and mark the separation of stages $1 \to 2$ and $2 \to 3$ with diamond and star, respectively. We take $\beta = 0.60$.

$\nu_{\rm loss} = 13$ km/s, corresponding to the benchmark case 2 as we will discuss below.

Figure 1 shows the density vs radius over time with (red) and without (blue) bulk cooling. Each curve is labeled with a Kn value for the innermost simulated shell. From the density evolution, we see the process can be divided into three stages. (i) Core expansion. Heat conduction is inwards ($L < 0$) and $Kn \gg 1$. The halo evolves quickly to a quasi-isothermal state. (ii) Self-similar collapse. Heat is conducted outwards ($L > 0$) and Kn slowly decreases. The self-similar collapse results in a cuspy density profile and with log-slope of approximately -2, a characteristic feature if the cooling is absent or mild. (iii) Post-self-similar collapse. Here $Kn < 1$ at the center and the inner density suddenly begins to increase dramatically. In Fig. 1, the symbol diamond denotes the $1 \to 2$ transition, when the innermost shell is at its least dense and its luminosity vanishes; the symbol star denotes the $2 \to 3$ transition, when $Kn = 1$.

For concreteness, we define a collapse time as the time at which $Kn = 0.1$ for the innermost shell, and we denote the collapse time with (without) inelastic cooling as t_c' (t_c). Since the evolution of the third stage is very fast, t_c' and t_c are largely determined by the time of the first two stages. The most important effect of the dissipative interaction is to significantly speed up the collapse time, $t_c' < t_c$. For LSB F583-1 with the model parameters chosen in Fig. 1, the collapse time with cooling is shortened by about a factor of 20, resulting in $t_c' \approx 8.5$ Gyr. This amount of cooling is disfavored, because the final density profile is too steep to be consistent with the observed profile of LSB F583-1 [33].

We perform a suite of simulations, varying the model parameters within the following range of values in dimensionless units: $\hat{\sigma} \equiv (\sigma/m)\rho_s r_s = 10^{-4}$–$10^{3}$, $\sigma'/\sigma = 10^{-3}$–1, and $\hat{\nu}_{\rm loss} \equiv \nu_{\rm loss}/(4\pi G\rho_s r_s^2)^{1/2} = 0$–5 with evenly log-spaced steps, and $\beta = 0.45$, 0.60, and 0.75. In Fig. 2 (left), we show results for the halo evolution with pure elastic self-scattering and no cooling. For $\hat{\sigma} \lesssim 1$, there is a simple scaling relation between $\beta\hat{t}_c \equiv \beta(4\pi G\rho_s)^{1/2} t_c$ and $\hat{\sigma}$, namely, $\beta\hat{t}_c \approx 150/\hat{\sigma}$, which can be expressed as

$$t_c \approx \frac{150}{\beta}\frac{1}{r_s\rho_s\sigma/m}\frac{1}{\sqrt{4\pi G\rho_s}}. \tag{3}$$

In this regime, a large $\hat{\sigma}$ speeds up the thermal evolution of the halo and shortens the collapse timescale. However, as $\hat{\sigma} \gtrsim 1$, the inverse proportionality is lost because the mean free path is too short and heat conduction is actually suppressed [46,53]. Below, when setting constraints on dissipative DM, we restrict to $\hat{\sigma} \le 0.1$, along with $\hat{\sigma}' \le \hat{\sigma} \le 0.1$, so that the mean free path is larger than the scale height for the halos we consider. Thus, the initial halo is in the optically thin regime and the cooling effect is mild. For the parameters shown in Fig. 1, $\hat{\sigma} = 0.1$ corresponds to $\sigma/m = 0.1/r_s\rho_s = 5.8$ cm^2/g, so the choice of $\sigma/m = 3$ cm^2/g satisfies the condition. Note we can recast the scaling relation in Eq. (3) as $t_c \propto r_s^{-1}\rho_s^{-3/2} \propto M_{200}^{-1/3} c_{200}^{-7/2}$, where M_{200} and c_{200} are the halo mass and concentration [54], respectively. Thus, t_c is extremely sensitive to c_{200}, which may have important implications for understanding dwarf galaxies in the Milky Way [55–58].

Our results are in good agreement with Ref. [50], where $\hat{\sigma} = 0.088$ and $\beta = 0.75$ were chosen. To compare with cosmological N-body simulations of dwarf halos in Ref. [27], we take the Pippin halo parameters, $r_s = 2.7$ kpc and $\rho_s = 1.73 \times 10^7\ M_\odot/\text{kpc}^3$, and apply Eq. (3). The estimated core-collapse time is $t_c \approx 80$ Gyr for $\sigma/m = 10$ cm^2/g and $t_c \approx 16$ Gyr for $\sigma/m = 50$ cm^2/g for $\beta = 0.60$, consistent with the absence of core collapse and the presence of a mild collapse, respectively, observed in the simulations. We also find that a

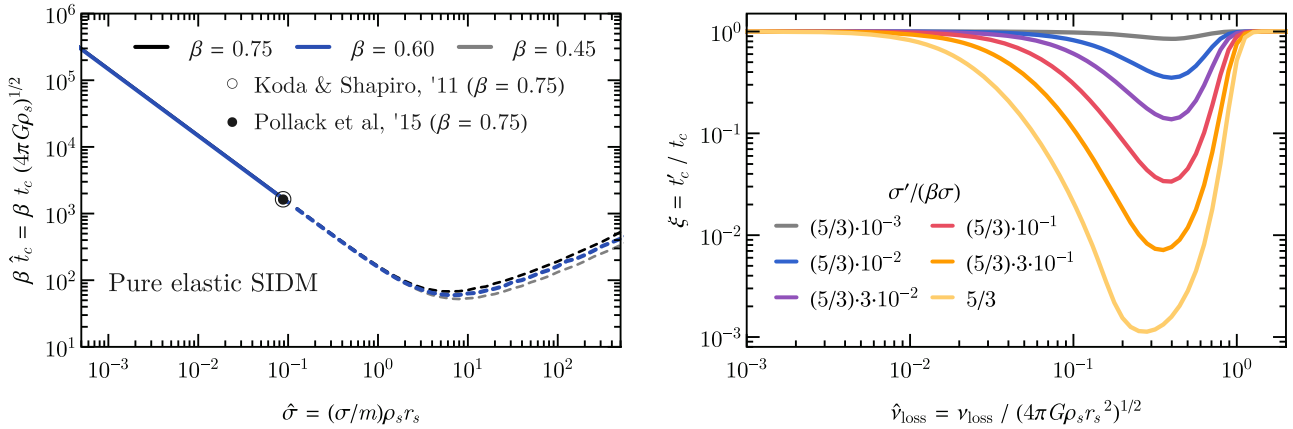

FIG. 2. Left: Dimensionless collapse time $\hat{t}_c$ multiplied by β as a function of $\hat{\sigma}$ when cooling is absent with $\beta = 0.75$ (black), 0.60 (blue), and 0.45 (gray). We also show the results recasted from N-body simulations [49] and fluid-model predictions [50], where $\beta = 0.75$ were used. In this work, we focus on $\hat{\sigma} \le 10^{-1}$ (solid). Right: Ratio of the collapse time, $\xi \equiv t_c'/t_c$, as a function of $\hat{\nu}_{\rm loss}$ for different values of $\sigma'/(\beta\sigma)$, where we take $\hat{\sigma} = 10^{-2}$ with $\beta = 0.60$. For the range of $\hat{\sigma} = 10^{-4}$–10^{-1} we have checked, $\sigma'/(\beta\sigma)$ well characterizes the $\xi - \hat{\nu}_{\rm loss}$ relation.

calibration with $\beta = 0.45$ yields a better agreement with the cosmological simulations.

Figure 2 (right) shows the reduction of the collapse time, $\xi \equiv t_c'/t_c$, from dissipative interactions. We find that the $\xi - \hat{\nu}_{\rm loss}$ relation is well characterized by $\sigma'/(\beta\sigma)$ for the test values, i.e., $\hat{\sigma} = 10^{-4}$–10^{-1} and $\beta = 0.45$–0.75. Overall, the maximal reduction is achieved when $\hat{\nu}_{\rm loss} \approx 0.3$ for a wide range of $\sigma'/(\beta\sigma)$.

The origin of this scale can be understood as the following: as the evolution starts, the cold inner halo ($r < r_s$) quickly thermalizes with the maximum velocity-dispersion of the initial NFW profile, which is about $\nu \sim 0.3(4\pi G\rho_s r_s^2)^{1/2}$ at $r = r_s$ [or $\hat{\nu} \equiv \nu/(4\pi G\rho_s r_s^2)^{1/2} \sim 0.3$], and stays near that value for most of the halo's evolution. For $\hat{\nu}_{\rm loss} \lesssim 0.3$, the energy loss is small per collision, while for $\hat{\nu}_{\rm loss} \gtrsim 0.3$, inelastic scattering can only occur among particles on the high-velocity tail or very late in the halo evolution (stage 3).

The collapse time in the presence of cooling is then $t_c' = \xi[\sigma'/(\beta\sigma), \hat{\nu}_{\rm loss}]t_c$, where t_c is given by Eq. (3) and ξ can be read from Fig. 2 (right). For $\hat{\nu}_{\rm loss} < 0.2$, we find an approximate formula $\xi \approx \exp[-\nu_{\rm loss}\sqrt{\sigma'/(\beta\sigma)}/0.035(4\pi G\rho_s r_s^2)^{1/2}]$. The collapse time can be reduced as much as a factor of 10^3, indicating that dissipative scattering can be important for the evolution of the SIDM halo. Compared to t_c, t_c' is also sensitive to $\nu_{\rm loss} = \hat{\nu}_{\rm loss}(4\pi G\rho_s r_s^2)^{1/2} \propto c_{200}^{1/2} M_{200}^{1/3}$.

Astrophysical implications.—For many dwarf and LSB galaxies, DM dominates the dynamics, and the stars and gas particles trace the gravitational potential well of the halo. Reference [33] analyzed the rotation curve data of 30 spiral galaxies and found that they can be fitted with an SIDM model with *elastic* self-scattering cross section $\sigma/m = 3$ cm^2/g. Among them, 18 of the galaxies have low baryon content and also exhibit a constant density core with no evidence of gravothermal collapse. We use this sample to constrain the dissipation parameters σ' and $\nu_{\rm loss}$ by demanding $t_c' > 10$ Gyr.

Figure 3 shows regions (shaded) where core collapse occurs in less than 10 Gyr for individual galaxies, taking halo parameters r_s and ρ_s from [33] as input. In these regions, the inner density profiles of the associated halos at 10 Gyr are much steeper than inferred from the stellar kinematics [33]; see Supplemental Material [42] for more details on determining the exclusion limits. In solid purple, we show the boundary from all galaxies imposing the constraint $t_c' < 10$ Gyr with calibration parameter $\beta = 0.60$; roughly the region with $0.1 \lesssim \sigma'/\sigma \lesssim 1$ and 10 km/s $\lesssim \nu_{\rm loss} \lesssim 100$ km/s is disfavored. We have checked the constraints are insensitive to the β values considered in the work; see Supplemental Material [42] for additional results with $\beta = 0.45$.

We explicitly demonstrate how the results in Fig. 2 can be used to derive the constraints in Fig. 3. Take LSB F583-1 as an example and focus on four benchmark points shown with small squares in Fig. 3. For pure elastic DM self-interactions with $\sigma/m = 3$ cm^2/g and $\beta = 0.60$, $t_c \approx 1.7 \times 10^2$ Gyr from Eq. (3), much longer than the age of the Universe. Taking $\sigma'/\sigma = 1$ and $\nu_{\rm loss} = 60$ km/s, $\hat{\nu}_{\rm loss} \approx 0.3$, so that $\xi \approx 10^{-3}$ from Fig. 2, resulting in a much shorter collapse time, $t_c' = \xi t_c \approx 0.2$ Gyr. Keeping $\sigma'/\sigma = 1$, and taking $\nu_{\rm loss} = 13$ km/s (135 km/s), so that $\hat{\nu}_{\rm loss} \approx 0.075$ (0.78), we find $\xi \approx 0.049(0.043)$ leads to $t_c' \approx 8.5(7.6)$ Gyr, which is disfavored. Finally, for $\sigma'/\sigma = 0.1$ and $\nu_{\rm loss} = 60$ km/s, we find $\hat{\nu}_{\rm loss} \approx 0.35$ and $\xi \approx 0.035$. This gives $t_c' \approx 6.3$ Gyr, which again is disfavored.

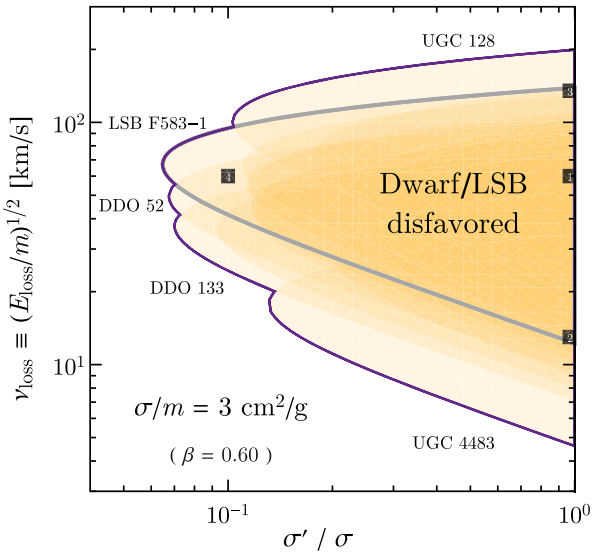

FIG. 3. Constraints on the dissipative parameters from the absence of core collapse in individual dwarf galaxies (yellow) within 10 Gyr and its overall boundary for the sample (purple). We take the fitted halo parameters of the galaxies from Ref. [33], also listed in the Supplemental Material [42] and labeled for the outer ones, and $\beta = 0.60$ in our fluid simulations. See text for detailed discussion on LSB F583-1 (gray) and the four benchmark cases (marked with numbers). We focus on the $\sigma'/\sigma \leq 1$ region, where the fluid model is applicable.

As an application, we consider the atomic DM model with hyperfine splitting transitions [11]. If the dark proton is the much heavier than the dark electron, $\nu_{\rm loss} = \sqrt{2E_{\rm hf}/m_p} = \sqrt{3/4}E_{\rm hf}/E_0 \approx 27$ km/s, where m_p is the dark proton mass, and $E_{\rm hf}/E_0 = 10^{-4}$ is the ratio of the hyperfine splitting to the binding energy. In this case, $\sigma/m_p \gtrsim 1$ cm^2/g on dwarf scales, and σ'/σ can be in the range of 0.1–1 for the dark structure constant ~0.02–0.08 and $m_p \sim 10$–60 GeV [11]. Thus, this model is subject to the constraints shown in Fig. 3. In addition, our results also put a lower limit on the threshold velocity, $\gtrsim$100 km/s, for dissipative SIDM models proposed to explain the formation of supermassive black holes [51].

Our constraints shown in Fig. 3 are based on $\sigma/m = 3$ cm^2/g. For models with different σ/m values, we can apply the same procedure to derive corresponding

constraints. Since the SIDM fits vary mildly for $\sigma/m = 1$–$10\ \mathrm{cm}^2/\mathrm{g}$ [36], we expect our method and results to have broad applications. In addition, we note that Ref. [33] has imposed strong constraints on the halo parameters r_s and ρ_s (M_{200} and c_{200}) from cosmological simulations [59] and the sample of the 18 galaxies we consider covers a wide range of halo concentration. Thus, our results are robust in the cosmological context.

Conclusions.—We have studied the gravothermal evolution of DM halos in the presence of dissipative DM self-interactions. After introducing a simple but well-motivated model to capture the cooling effect, we performed numerical simulations and obtained numerical templates between the core-collapse time and the model parameters, which can be easily adapted for specific particle physics realizations of dissipative DM. Utilizing the density cores inferred from the dwarf galaxies, we put strong constraints on the dissipation parameters. Our results have been overall confirmed by recent N-body simulations with dissipative SIDM [51]. It is of interest to generalize our analysis to include velocity-dependent cross sections, which we leave for future work. Our formalism can be extended also to other scenarios, e.g., those proposed in Refs. [60–63], where DM particles are heated from energy release due to dark-sector interactions, which could further increase the core size of the halo and lower its central density.

We thank Jun Koda and Paul Shapiro for providing many insights on the fluid simulations as well as additional information on their N-body simulations. We also thank Jason Pollack for helpful discussions on the fluid simulations, as well as Prateek Agrawal, Joseph Bramante, Francis-Yan Cyr-Racine, Manoj Kaplinghat, Julio Navarro, Annika Peter, Ben Safdi, Martin Schmaltz, Neelima Sehgal, Scott Tremaine, and Sean Tulin for useful discussions. The authors thank the KITP at UCSB for hospitality, where their research was supported by the National Science Foundation under Grant No. NSF PHY-1748958. H. B. Y. acknowledges the T. D. Lee Institute, Shanghai, and Y. Z. thanks the Aspen Center for Physics, for hospitality during the completion of this work. R. E. acknowledges support from U.S. Department of Energy under Grant No. DE-SC0017938. S. D. M. was supported by the Fermi Research Alliance, LLC under Contract No. DE-AC02-07CH11359 with the U.S. Department of Energy, Office of Science, Office of High Energy Physics. H. B. Y. acknowledges support from U.S. Department of Energy under Grant No. DE-SC0008541 and a UCR Regents' Faculty Development Award. Y. Z. acknowledges support from U.S. Department of Energy under Grant No. DE-SC0015845. The U.S. Government retains and the publisher, by accepting the article for publication, acknowledges that the U.S. Government retains a non-exclusive, paid-up, irrevocable, world-wide license to publish or reproduce the published form of this manuscript, or allow others to do so, for U.S. Government purposes.

*ymzhong@bu.edu

[1] M. Battaglieri *et al.*, arXiv:1707.04591.
[2] J. Alexander *et al.*, arXiv:1608.08632.
[3] R. Essig *et al.*, Working group report: New light weakly coupled particles, in *Proceedings of the 2013 Community Summer Study on the Future of U.S. Particle Physics: Snowmass on the Mississippi (CSS2013): Minneapolis, MN, USA, 2013* (2013), http://www.slac.stanford.edu/econf/C1307292/docs/IntensityFrontier/NewLight-17.pdf.
[4] S. Tulin and H.-B. Yu, Phys. Rep. **730**, 1 (2018).
[5] D. E. Kaplan, G. Z. Krnjaic, K. R. Rehermann, and C. M. Wells, J. Cosmol. Astropart. Phys. 05 (2010) 021.
[6] F.-Y. Cyr-Racine and K. Sigurdson, Phys. Rev. D **87**, 103515 (2013).
[7] J. M. Cline, Z. Liu, G. D. Moore, and W. Xue, Phys. Rev. D **89**, 043514 (2014).
[8] K. K. Boddy, J. L. Feng, M. Kaplinghat, Y. Shadmi, and T. M. P. Tait, Phys. Rev. D **90**, 095016 (2014).
[9] D. P. Finkbeiner and N. Weiner, Phys. Rev. D **94**, 083002 (2016).
[10] R. Foot and S. Vagnozzi, Phys. Rev. D **91**, 023512 (2015).
[11] K. K. Boddy, M. Kaplinghat, A. Kwa, and A. H. G. Peter, Phys. Rev. D **94**, 123017 (2016).
[12] K. Schutz and T. R. Slatyer, J. Cosmol. Astropart. Phys. 01 (2015) 021.
[13] Y. Zhang, Phys. Dark Universe **15**, 82 (2017).
[14] M. Blennow, S. Clementz, and J. Herrero-Garcia, J. Cosmol. Astropart. Phys. 03 (2017) 048.
[15] A. Das and B. Dasgupta, Phys. Rev. D **97**, 023002 (2018).
[16] D. Lynden-Bell and R. Wood, Mon. Not. R. Astron. Soc. **138**, 495 (1968).
[17] C. S. Kochanek and M. White, Astrophys. J. **543**, 514 (2000).
[18] R. A. Flores and J. R. Primack, Astrophys. J. **427**, L1 (1994).
[19] B. Moore, Nature (London) **370**, 629 (1994).
[20] G. Gentile, P. Salucci, U. Klein, D. Vergani, and P. Kalberla, Mon. Not. R. Astron. Soc. **351**, 903 (2004).
[21] M. Persic, P. Salucci, and F. Stel, Mon. Not. R. Astron. Soc. **281**, 27 (1996).
[22] R. Kuzio de Naray, S. S. McGaugh, and W. J. G. de Blok, Astrophys. J. **676**, 920 (2008).
[23] W. J. G. de Blok, F. Walter, E. Brinks, C. Trachternach, S-H. Oh, and R. C. Kennicutt, Astron. J. **136**, 2648 (2008).
[24] S.-H. Oh, W. de Blok, E. Brinks, F. Walter, and R. C. Kennicutt, Astron. J. **141**, 193 (2011).
[25] S.-H. Oh *et al.*, Astron. J. **149**, 180 (2015).
[26] M. Vogelsberger, J. Zavala, and A. Loeb, Mon. Not. R. Astron. Soc. **423**, 3740 (2012).
[27] O. D. Elbert, J. S. Bullock, S. Garrison-Kimmel, M. Rocha, J. Oñorbe, and A. H. G. Peter, Mon. Not. R. Astron. Soc. **453**, 29 (2015).
[28] D. N. Spergel and P. J. Steinhardt, Phys. Rev. Lett. **84**, 3760 (2000).
[29] C. Firmani, E. D'Onghia, G. Chincarini, X. Hernandez, and V. Avila-Reese, Mon. Not. R. Astron. Soc. **321**, 713 (2001).
[30] R. Dave, D. N. Spergel, P. J. Steinhardt, and B. D. Wandelt, Astrophys. J. **547**, 574 (2001).

[31] M. Rocha, A. H. G. Peter, J. S. Bullock, M. Kaplinghat, S. Garrison-Kimmel, J. Oñorbe, and L. A. Moustakas, Mon. Not. R. Astron. Soc. **430**, 81 (2013).
[32] J. Zavala, M. Vogelsberger, and M. G. Walker, Mon. Not. R. Astron. Soc. **431**, L20 (2013).
[33] A. Kamada, M. Kaplinghat, A. B. Pace, and H.-B. Yu, Phys. Rev. Lett. **119**, 111102 (2017).
[34] M. Kaplinghat, S. Tulin, and H.-B. Yu, Phys. Rev. Lett. **116**, 041302 (2016).
[35] M. Valli and H.-B. Yu, Nat. Astron. **2**, 907 (2018).
[36] T. Ren, A. Kwa, M. Kaplinghat, and H.-B. Yu, Phys. Rev. X **9**, 031020 (2019).
[37] J. J. Fan, A. Katz, L. Randall, and M. Reece, Phys. Rev. Lett. **110**, 211302 (2013).
[38] M. R. Buckley, J. Zavala, F.-Y. Cyr-Racine, K. Sigurdson, and M. Vogelsberger, Phys. Rev. D **90**, 043524 (2014).
[39] G. D'Amico, P. Panci, A. Lupi, S. Bovino, and J. Silk, Mon. Not. R. Astron. Soc. **473**, 328 (2018).
[40] M. R. Buckley and A. DiFranzo, Phys. Rev. Lett. **120**, 051102 (2018).
[41] N. J. Outmazgine, O. Slone, W. Tangarife, L. Ubaldi, and T. Volansky, J. High Energy Phys. 11 (2018) 005.
[42] See Supplemental Material at http://link.aps.org/supplemental/10.1103/PhysRevLett.123.121102 for calibration of the fluid model with isolated and cosmological *N*-body simulations.
[43] D. Lynden-Bell and P. Eggleton, Mon. Not. R. Astron. Soc. **191**, 483 (1980).
[44] L. S. Spitzer, Jr., *Dynamical Evolution of Globular Clusters* (Princeton University Press, Princeton, NJ, 2014), Vol. 799.
[45] J. Binney and S. Tremaine, *Galactic Dynamics: Second Edition*, Princeton Series in Astrophysics (Princeton University Press, Princeton, NJ, 2011).
[46] O. Y. Gnedin and J. P. Ostriker, Astrophys. J. **561**, 61 (2001).
[47] S. Balberg and S. L. Shapiro, Phys. Rev. Lett. **88**, 101301 (2002).
[48] S. Balberg, S. L. Shapiro, and S. Inagaki, Astrophys. J. **568**, 475 (2002).
[49] J. Koda and P. R. Shapiro, Mon. Not. R. Astron. Soc. **415**, 1125 (2011).
[50] J. Pollack, D. N. Spergel, and P. J. Steinhardt, Astrophys. J. **804**, 131 (2015).
[51] J. Choquette, J. M. Cline, and J. M. Cornell, J. Cosmol. Astropart. Phys. 07 (2019) 036.
[52] J. F. Navarro, C. S. Frenk, and S. D. M. White, Astrophys. J. **490**, 493 (1997).
[53] P. Agrawal, F.-Y. Cyr-Racine, L. Randall, and J. Scholtz, J. Cosmol. Astropart. Phys. 05 (2017) 022.
[54] J. F. Navarro, C. S. Frenk, and S. D. M. White, Astrophys. J. **462**, 563 (1996).
[55] H. Nishikawa, K. K. Boddy, and M. Kaplinghat, arXiv:1901.00499.
[56] M. Kaplinghat, M. Valli, and H.-B. Yu, arXiv:1904.04939.
[57] O. Sameie, H.-B. Yu, L. V. Sales, M. Vogelsberger, and J. Zavala, arXiv:1904.07872.
[58] F. Kahlhoefer, M. Kaplinghat, T. R. Slatyer, and C.-L. Wu, arXiv:1904.10539.
[59] A. A. Dutton and A. V. Macciò, Mon. Not. R. Astron. Soc. **441**, 3359 (2014).
[60] S. D. McDermott, Phys. Rev. Lett. **120**, 221806 (2018).
[61] M. I. Gresham, H. K. Lou, and K. M. Zurek, Phys. Rev. D **98**, 096001 (2018).
[62] M. Vogelsberger, J. Zavala, K. Schutz, and T. R. Slatyer, arXiv:1805.03203.
[63] X. Chu and C. Garcia-Cely, J. Cosmol. Astropart. Phys. 07 (2018) 013.